Astron. Astrophys. 238, 315–324 (1990)

ASTRONOMY
AND
ASTROPHYSICS

Scanning interferometer observations of the shell N 186E in the Large Magellanic Cloud *

M. Rosado [1], A. Laval [2], J. Boulesteix [2], Y.P. Georgelin [2], A. Greve [3], M. Marcelin [2], E. Le Coarer [2], and A. Viale [2]

[1] Universidad Nacional Autonoma de Mexico, Instituto Astronomia, Apartado Postal 70-264, Ciudad Universitaria, CP-04510 Mexico, D.F.
[2] Observatoire de Marseille, 2, Place Le Verrier, F-13248 Marseille Cedex 04, France
[3] IRAM, 300 rue de la Piscine, Domaine Universitaire, F-38406 St. Martin d'Hères Cedex, France

Received February 14, accepted May 3, 1990

Abstract. The velocity field and the Hα flux of the large shell N186E of the LMC are measured over a $7' \times 7'$ field, covering most of the filamentary structure. The radial velocity field appears to be contamined by faint blue-shifted and red-shifted emission which confirms the presence of H I slabs along the line of sight. The remaining gas in N186E does not show high velocity expansion motions ($25\,km\,s^{-1}$), much less than found inside the similar but smaller bubble N185. The recently detected exciting stars are sufficient to explain the ionization of N186E, although none of them is located close to the centre.

The density inside the filaments is produced by weak shocks, whereas the circular shape and the size of the shell indicate homogeneity of the preshock material. An intense interaction is found at the dense border between N186E and the young neighbouring SNR, N186D. N186E is probably an old SNR, now being ionized by internal stars.

Key words: interstellar shells – kinematics and dynamics of interstellar medium – galaxies: Magellanic Clouds

1. Introduction

The study of the origin of large diameter (50–200 pc) bubbles in the LMC with intermediate [S II]/Hα line-ratios and internal hot stars has been the subject of several publications (Chu, 1983; Lasker, 1980; Meaburn, 1987; Rosado, 1986). These authors investigated whether they originate from explosions or stellar winds. On the one hand, the discrimination of SNRs has progressed by means of the radio observations, by recent X-ray observations with the Einstein Satellite, and the development of more sophisticated optical observations. On the other hand, the detailed knowledge of the young stellar content in bubbles together with studies of their kinematics proved to be crucial for clarifying the origin of the nebulae. Since 1980, we are engaged to improve our knowledge of shells and bubbles by high-sensitivity optical observations. In this context we have studied Henize's (1956) nebula N186E by applying the CIGALE FP scanning interferometer equipment (Boulesteix et al., 1984; Marcelin et al., 1985).

This nebula has been photographed in Hα + [N II], Hα and [S II] emission lines by Davies et al. (1976), Lasker (1979), and Meaburn et al. (1984), respectively. The photographs reveal a ring-shaped nebula of $9'.2 \times 6'.8$ angular dimension corresponding to a mean linear diameter of 128 pc at a distance of 55 kpc for the LMC (Feast, 1984); the SNR N186D is located at the northern edge of the bubble N186E. Both nebulae form the complex DEM 50 (Davies et al., 1976). The SNR has been studied earlier (Laval et al., 1989, hereafter Paper I) under identical conditions.

We have shown in Paper I that both nebulae (the SNR and the bubble) are located in the same H I slab moving at about $240\,km\,s^{-1}$ (heliocentric velocity) and that they are probably interacting at their common boundary through an induced secondary shock of $50\,km\,s^{-1}$ velocity. The remaining part of the SNR expands spherically with a velocity of $90\,km\,s^{-1}$. The monochromatic photographs reveal that the [S II]/Hα line-ratios of the bubble and the SNR are similar (Lasker, 1977, found a [S II]/Hα line-ratio of 1 for N186E). When compared with the SNR, the [O III] emission of the bubble is fainter (if not absent).

A small X-ray source of IPC flux of $0.0005\,count\,s^{-1}\,arcmin^2$ have been detected from this bubble, located near the brighter X-ray emission of the SNR N186D (Mathewson et al., 1983). The position of this small X-ray source coincides with a FIR source detected by IRAS and possibly indicating re-radiation by dust grains of the emission from a luminous early-type star (Graham et al., 1987) and with a small association of early-type stars studied photometrically by Greve et al. (1988). The spatial coincidence suggests that the FIR source is excited by the stellar association, as will be examined below.

In this publication we present the results of observations performed with the scanning FP interferometer (CIGALE) attached to the 1.5 m ESO telescope and operated under the same conditions as the observations of the bubble N62A described by Laval et al. (1987). We refer to the earlier paper and to Marcelin

Send offprint requests to: A. Laval

* Based on observations collected at the European Southern Observatory, ESO, Chile

et al. (1985) for a general description of the observations and data reduction.

From the CIGALE observations of N186E we derive the kinematical field (Sect. 2) and the density of the bubble (Sect. 3). The stellar content of the bubble is described in Sect. 4. Combining this information allows us to clarify the origin of the nebula (Sect. 5).

2. Kinematical data

Figure 1 is a reproduction of an Hα + [N II] photograph published by Meaburn et al. (1984); we have inserted the square shaped field of our observation. Some filamentary regions at the boundary of the bubble are not included in our field (because of the size of the employed interferential filter which limits the field of view to 7′). The field marked in Fig. 1 is observed with a spatial resolution of $2''.6 \times 2''.6$ or $0.7 \times 0.7\,pc^2$ at the LMC distance. The field is analysed with a free spectral range of 8.2 Å (or 376 km s^{-1}) scanned in 20 steps (giving 20 velocity channels). Each computed wavelength channel covers one slice of 0.41 Å (or 18.8 km s^{-1}). The total exposure time was 6800 s. Figure 2 shows several examples of the Hα emission as detected in the CIGALE monochromatic maps (hereafter called λ-maps) corresponding to four wavelength channels centered at $\lambda = 6566.5$ Å (169 km s^{-1}), $\lambda = 6568.1$ Å (244 km s^{-1}), $\lambda = 6569.0$ Å (282 km s^{-1}), and $\lambda = 6569.4$ Å (301 km s^{-1}). While the three last maps display prominent features covering the whole field, the map corresponding to channel 10 contains only one bright feature, which is probably due to the interaction between the SNR N186D and the bubble (see Paper I).

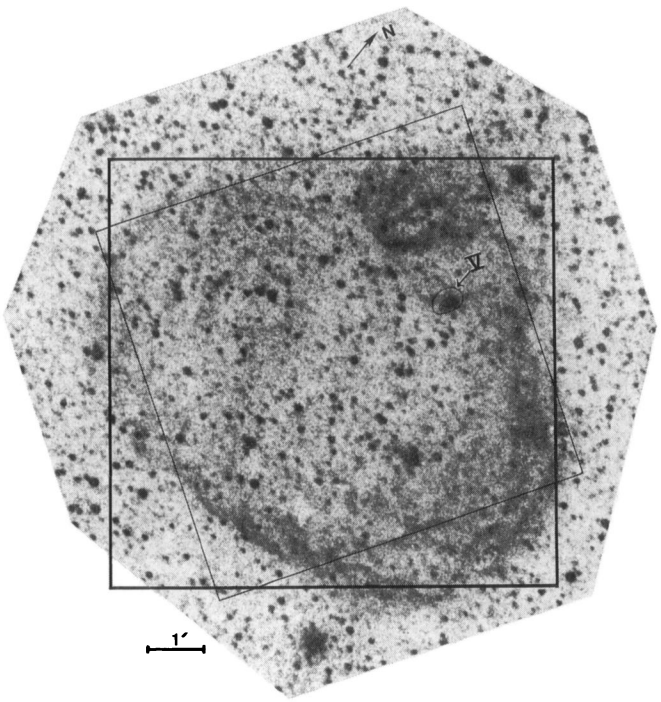

Fig. 1. Field of the CIGALE observations superimposed on the Hα + [N II] photograph taken by Meaburn et al. (1984). The heavy frame is the central part of the field of view of the IPCS. The thin frame (the tilted one) corresponds to the useful field, limited by the interferential filter

The results of the kinematic analysis are presented in Figs. 3–5. The heliocentric velocity is used throughout this paper. Figure 3 shows the averaged values of the velocity and the velocity dispersion for characteristic features appearing in the maps of Fig. 2. The determination of each average velocity is based on the barycenter method with a precision of 6.3 km s^{-1} (Laval et al., 1987). The field is characterized by many zones with high velocity dispersions of $15\,km\,s^{-1} \leqq \sigma \leqq 65\,km\,s^{-1}$. The filaments at the edges have the lowest velocity dispersions of 6 to 13 km s^{-1}; however their central heliocentric velocities vary between 231 km s^{-1} at the NE and 244 km s^{-1} at the SW. To obtain spatial information of the velocities, we separate the local components by Gaussian profiles fitting. Figure 4 shows some examples of the profile shapes and of the locations across the nebula. (Note that at the projected edges where the intensity looks higher, no composite profile is found but a single Gaussian curve as expected from the dispersion.) Figure 5 shows the velocity value of the different Gaussian components. We find a main component at a mean wavelength of 6568.0 ± 0.2 Å (corresponding to velocities between 222 and 244 km s^{-1}) which covers the entire field of observation. This component has a highly variable intensity ($4 < S/N < 33$) (Fig. 2, channel 14); the Hα intensities have been measured for the 30 zones of Fig. 5, (see Sect. 3). We find a second velocity component at 6569.2 Å ± 0.4 Å (corresponding mainly to velocities between 275 and 310 km s^{-1}) in 23 specific locations, essentially filaments, with $2 < S/N \leqq 19$; they are seen in Fig. 2, channels 16 and 17. We can give only an upper limit for the 7 other areas. Finally, we detect a third velocity component at 6566.8 ± 0.3 Å (corresponding to a velocity range from 172 to 199 km s^{-1} with a mean value of 185 ± 9 km s^{-1}) in the profiles of the 23 zones of moderate or faint emission, the S/N ratio varies from 1.7 to 6. It is possible that in zones of higher emission this component is masked by the wings of the stronger components, so that its detection is impossible.

We find a single dense knot inside the bubble (V in Fig. 1). Its velocity is 229 km s^{-1} for S/N = 55. Only four velocity points cover the small dimension of the intense part ($\phi \simeq 5''$). The velocity dispersion of $\leqq 7$ km s^{-1} is equal to the theoretical resolution of the CIGALE equipment (Laval et al., 1987). The line profile does not indicate turbulent motion.

3. Monochromatic emission

The Hα intensities could be derived from the number of events registered for each pixel, once the process of conversion into physical flux units has been established. However it is possible to derive relative intensities in case the absolute calibration is not available. This is the case for N186 which was not included in the previous Hα photometric observations of the LMC (Caplan and Deharveng, 1985).

There are several sources of uncertainty (Laval et al., 1987). When several velocity components are present, an uncertainty is introduced by the choice of the continuum levels of the components. Since we do not know the relative importance of the different continuum levels and their velocities, and since the Perot-Fabry transmission is never quite null, the precise instrumental response cannot be established within the field of observation. It is difficult to quantity the final error in the observation of N186, but we may expect that at certain positions the error may reach 30% of the measured intensity. Nevertheless, in order to compare the observations with models of shocked layers covering a wide range of densities, an estimate of the Hα fluxes is obtained in the

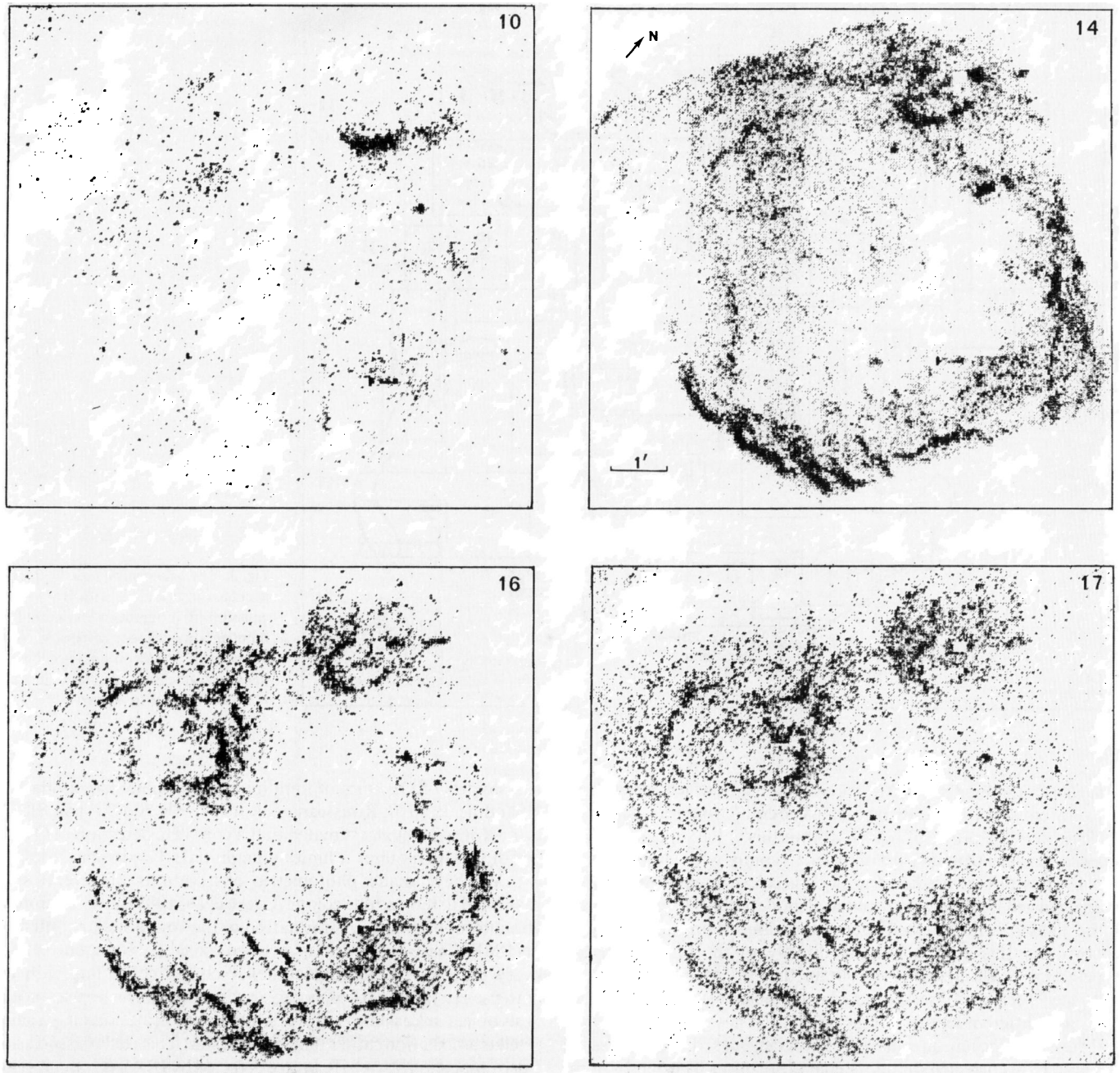

Fig. 2. N 186 E and N 186 D reconstructed from the CIGALE λ-maps. The λ-maps correspond to narrow monochromatic slices, of 0.41 Å width. The slices 10, 14, 16, and 17 correspond to heliocentric radial velocities of 169 ± 9, 244 ± 9, 282 ± 9, and 301 ± 9 km s^{-1}. The stars are eliminated

following way. Three additional fields were observed with CIGALE during the same observing run. Each field contains a nebula of the list of objects with absolute Hα flux measurement by Caplan and Deharveng (1983). The comparison of the CIGALE measurements and the Hα fluxes measured by Caplan and Deharveng gives the calibration factor. This indirect process of calibration introduces severe additional assumptions and cumulative errors resulting from the different instrumental response, atmospheric transmission, the presence of several gaseous layers inside the calibrating fields. The precison of the average calibration factor will be not better than 35%. Hence, the estimated total uncertainty of the flux values may reach $\pm 50\%$. Such difficulties should be minimized with the complete Hα survey of the Magellanic Clouds planned for 1991 with CIGALE through fields of 40′ of diameter.

With the present conditions we derive for N 186 E a Hα flux of $2.5\ 10^{-11}$ erg cm^{-2} s^{-1} integrated over 49 (arcmin)^2 (this Hα flux does not include the region of interaction with the SNR N 186 D). Adopting an average colour excess of $E_{B-V} = 0.10$ mag (see Sect. 4) for the interstellar absorption, the reddening corrected Hα

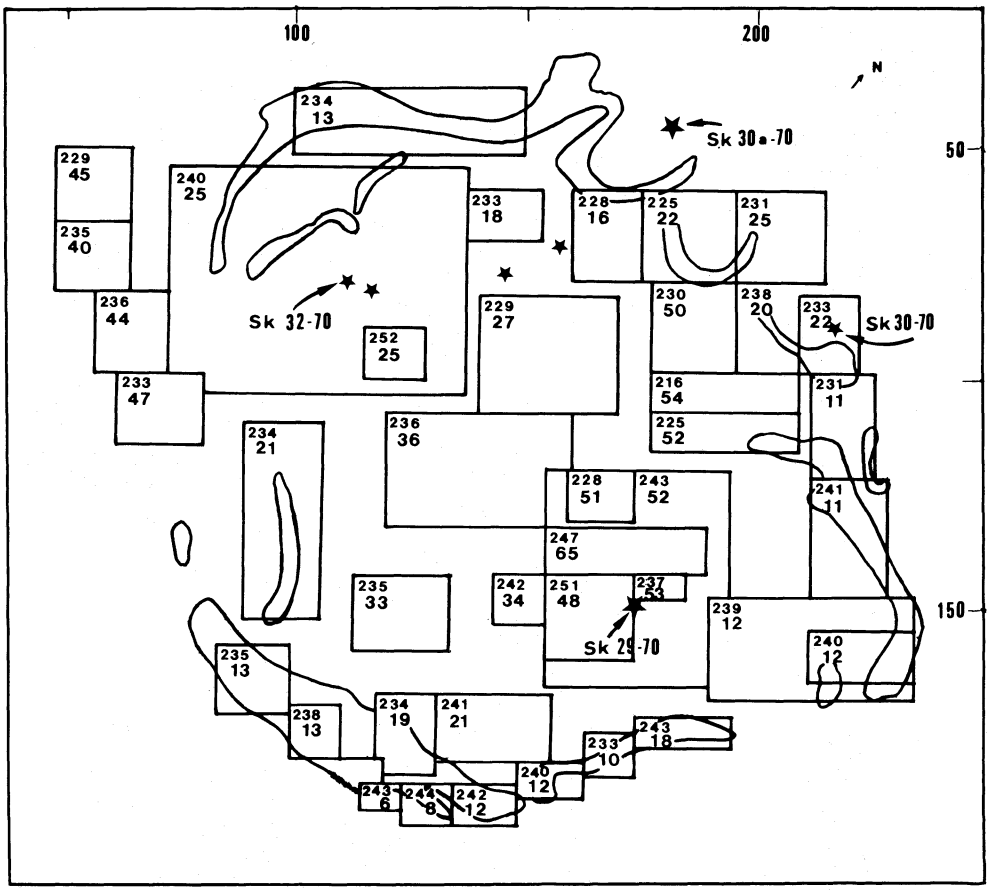

Fig. 3. The heliocentric radial velocities averaged over regions with Hα emission (first number). The second number is the velocity dispersion. Both are in km s^{-1}. The outlines are the nebular filaments. The stars visible on Hα observations are shown

surface brightness is 0.9 10^{-5} erg cm^{-2} s^{-1} sr^{-1} which corresponds to an emission measure EM of 64 pc cm^{-6} when assuming an electron temperature of 6000 K. From this value we compute the mean rms electron density in order to compare the ionization of N186E with that predicted for a classical Strömgren sphere. For an idealized homogeneous spherical model (while an estimation of the thickness in the shell model is so uncertain, and although obviously this does not apply directly to the filamentary appearance of the nebula) we obtain the rms electron density of 0.7 cm^{-3} for the observed nebular diameter of 128 pc.

For different features of the nebula Table 1 gives the observed fluxes, and root mean square electron densities. The Hα fluxes of Table 1 are corrected for interstellar absorption. The depths of the features, Δl, along the line of sight is assumed to be equal to their width in the monochromatic maps.

Table 2 gives the Hα fluxes of the three components identified in Fig. 5. For the main, blue shifted and red shifted velocity components the entries of Table 2 are:

– Column 1: position coordinates of the upper left and lower right corners of the rectangular windows defined in Fig. 5;

– Columns 2–4: Hα surface brightness and FWHM of the corresponding Gaussian component. The FWHM of the nebular emission profile is given in case it exceeds the instrumental profile of 42 km s^{-1}.

4. Stellar content

The available catalogues do not report all of the early-type stars embedded in the nebulae. Two blue stars are listed in the catalogues of OB stars of limiting photographic magnitude 12.5 (Sanduleak, 1970; Rousseau et al., 1978): SK 30a-70° and SK 32-70°. Rousseau et al. estimated that a complete detection of O stars of the LMC requires a limiting magnitude $V = 16$ mag.

We have made photometric observations of several stars assumed to have a blue colour (Greve et al., 1988), in an attempt to obtain supplementary information of the young stellar content of N186E. These observations revealed three blue stars, one being a very blue star in a compact stellar cluster coinciding with the intense Hα knot marked as region *V* in Fig. 1. The appearance of this object in Lasker's (1977) photograph indicates that it is a small stellar association rather than a single star. This stellar association also coincides with a FIR source detected by IRAS (Graham et al., 1987) and with the X-ray source (Mathewson et al., 1983) already mentioned in Sect. 1. In the following we will denote this stellar association as Gr 3. The IRAS source has an estimated total luminosity of $1.1 \times 10^5\ L_\odot$ and may be powered by a single O_4 star or several stars of later spectral types (Graham et al., 1987). This is in agreement with the photometric data of Gr 3 (Table 3).

Table 3 gives the parameters of the five bluest and brightest stars or associations in the field. Column 1 gives the identification of the star from Sanduleak (1970) or Greve et al. (1988). Columns 2–4 are the V magnitude, the extinction A_V and the absolute magnitude M_V. Column 5 is either the known spectral type from Rousseau et al. (1978) or the spectral type estimated from the photometry (in brackets). Column 6 is the excitation parameter as given by Panagia (1973), corresponding to the spectral type. If we assume N186E to be a homogeneous Strömgren sphere, the existing internal stars are sufficient to account for the ionization of

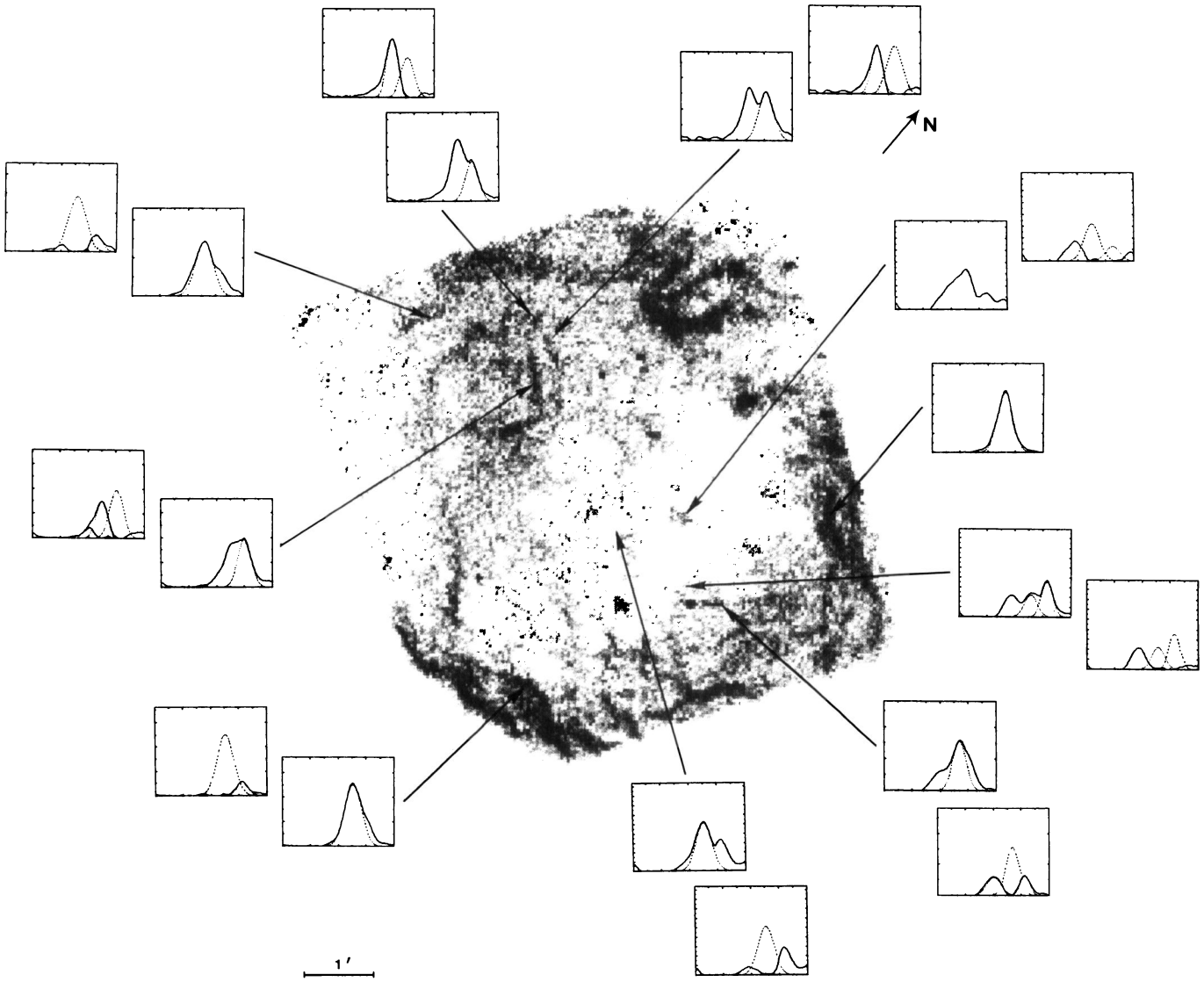

Fig. 4. Hα profiles superimposed on the monochromatic Hα map. The profiles are shown before (—) and after (----) decomposition into Gaussian profiles. The scale is normalized to the peak value inside each graph

this shell. Indeed, the lower limit of the excitation parameter corresponding to the total available UV stellar flux (Table 3) is 135 pc cm^{-2} (when decomposing Gr 3 for instance either in 40 stars with $M_V = -4.5$ or 5 stars with $M_V = -6.8$). On the other hand, the nebular excitation parameter is: $U = R\langle n_e^2\rangle^{1/3} =$ 50 pc cm^{-2} when we adopt $R = 64$ pc and $\sqrt{\langle n_e^2\rangle} = 0.7$ cm^{-3} (Table 1).

Consequently, the number of UV photons emitted only by Gr 3 is sufficient to ionize a homogeneous sphere of the size of this shell. However when comparing homogeneous and two-component models of H II regions (Stasińska, 1982), we find that our evaluation underestimates the number of ionizing photons required for a two-component model when keeping the other parameters (metallicity, etc....) constant. However, the potential of excitation by Gr 3 is so large (Table 3) that the H II shell is probably ionized by these stars (although none of them is located near the center of the bubble as seen in Fig. 1). Anyhow, we have assumed that these stars are located in the nebulae. This seems plausible for the brightest stars SK 32-70° and Gr 3 which are surrounded by filaments and an ionized knot. On the other hand, the fainter stars Gr 1 and Gr 2 may not be associated with the nebula.

The star SK 32-70° has been observed by IUE (Nandy et al., 1981). Being a supergiant a stellar wind is expected to be present, although this feature is not mentioned by Nandy et al.

For evaluating the mean extinction $A_{H\alpha}$ along the line of sight, we have used four of the stars listed in Table 2, and SK 30-70°, a B_5I star with a colour excess of 0.13 mag (Rousseau et al., 1978). We consider the extinction of the reddened stellar complex Gr 3 as not being representative of the general extinction of the nebula. Besides the existence of associated FIR emission, the stars Gr 3 may be highly reddened luminous stars embedded in denser cloudlets or circumstellar shells (Greve et al., 1988). We derive a mean extinction $A_{H\alpha} = 0.24$ mag.

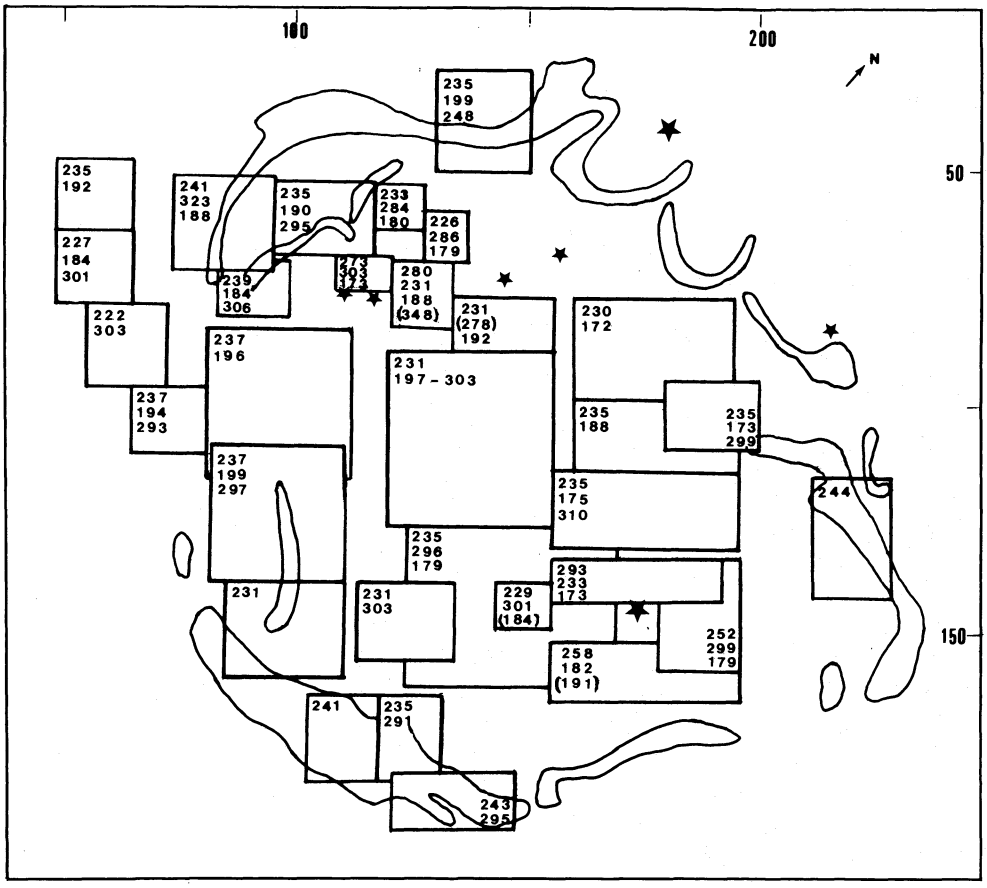

Fig. 5. Velocities of the different profile components (in km s^{-1}). The velocities are ordered for decreasing intensity

Table 1. Hα fluxes and densities in N186E

	Hα flux (erg cm^{-2} s^{-1})	Area (arcmin)^2	E.M. (cm^{-6} pc)	Δl (pc)	$\sqrt{\langle n_e^2 \rangle}$ (cm^{-3})
H II bubble (average)	30.5 10^{-12}	49.00	70	128	0.7
Edges of the shell	5.0	4.86	110	20	2
Surroundings of Sk 32-70°	4.5	5.21	95	38	1.5
High-velocity filament close to SK 32-70°	0.6	0.72	85	1.5–2	7
Condensation *V* (average)	0.3	0.11	340	5	8
Condensation *V* (core)	0.1	0.008	2000	1.5	35

5. Interpretation of the observations

As demonstrated in Sect. 2 of the F.P. observations, we distinguish three velocity components: an intense component at 222–244 km s^{-1} (average integrated intensity of $0.7 \pm 0.4\ 10^{-5}$ erg cm^{-2} s^{-1} sr^{-1}) and two faint components at 275–310 km s^{-1} (average integrated intensity of $2.2 \pm 2.0\ 10^{-6}$ erg cm^{-2} s^{-1} sr^{-1}) and 172–199 km s^{-1} (average integrated intensity of $1.4 \pm 0.5\ 10^{-6}$ erg cm^{-2} s^{-1} sr^{-1}), respectively.

Both faint components vary slowly across the nebula although without any correlation of their distance to a possible center (Table 2). The gas distribution in the faint components is more homogeneous than that of the filamentary main component.

The spatial distribution of the main component confirms that N186E is a shell, with the highest fluxes occurring at the periphery.

Multiple component profiles were also found in the velocity data of SNR N186D located at the North of this shell (Paper I).

Table 2. Variations of the Hα fluxes inside the gaseous components. The position is defined by the pixel coordinates of the opposite corners for each rectangular zone of Figs. 2 and 5. The area is in (arcsec)^2. The fluxes are given in erg cm^{-2} s^{-1} sr^{-1}, the FWHM in km s^{-1}

Position X_1, Y_1, X_2, Y_2	Area	Main component	FWHM	Blue shifted component	FWHM	Red shifted component	FWHM
48, 48, 64, 64	1969	0.50 10^{-5}		0.20 10^{-5}		– 10^{-5}	
48, 64, 64, 80	1969	0.45		0.10		0.10	
56, 80, 72, 96	1969	0.65	85	–		0.20	
64, 96, 80, 112	1969	0.30		0.25		0.20	
74, 54, 94, 74	2981	0.85	75	0.05		0.15	
80, 85, 119, 100	7085	0.90	62	0.15		–	
80, 110, 110, 140	6546	0.60		0.15		0.05	
85, 70, 100, 82	1406	0.85	56	0.20		0.20	
85, 141, 110, 160	3542	0.75	58	–		–	
95, 53, 117, 68	2488	1.00		0.15		0.15	
97, 168, 113, 184	1969	1.70	62	–		–	
113, 141, 128, 156	1744	0.70	64	–		0.25	
117, 170, 130, 184	1431	1.40	71	–		0.20	
118, 53, 128, 61	669	0.85		0.15	60	0.65	
120, 70, 135, 85	1731	0.55		0.10		0.75	
120, 90, 155, 128	9564	0.60		0.10		0.10	
120, 182, 152, 195	3147	1.60	60	–		0.15	
122, 129, 170, 165	12256	0.50	66	0.05	62	0.20	
128, 59, 138, 71	967	0.60		0.10		0.75	64
130, 30, 150, 50	3004	0.75		0.15		0.05	
136, 80, 155, 90	1499	0.60		0.05		0.15	
144, 142, 155, 153	981	0.50	70	0.05		0.15	
155, 117, 195, 135	5307	0.30	60	0.15	66	0.10	
155, 136, 192, 148	3389	0.20		0.20	56	0.25	
155, 153, 195, 167	4157	0.90	66	0.10		0.15	
160, 80, 195, 98	4659	0.75		0.10	94	–	
160, 99, 195, 116	4414	0.30		0.15		0.50	
177, 136, 195, 165	3853	0.70	56	0.20	62	0.20	
181, 97, 200, 112	2180	0.20		0.25	66	0.10	
212, 121, 229, 145	3065	1.90		–		–	

Table 3. Blue internal stars. The excitation parameter U is in pc cm^{-2}

*	V	A_V	M_V	Sp	U
Sk 30a-70°	13.46	0.37	−6.6	B1:	11.2
Sk 32-70°	13.10	0.06	−6.6	B0I	43.2
Gr 3	11.58	1.46	−8.5	(O9V-O5I)	135–189
Gr 1	14.66	0.41	−4.4	(B2III-II)	–
Gr 2	14.46	0.16	−4.6	(B0.5III-B1II)	11

We conclude from the arguments based on intensities that the detected components indicate internal motion of the SNR despite the existence of H I slabs at the same velocities (Meaburn et al., 1984).

In case of N 186 E, the situation is quite different: the intensities and spatial positions of the velocity components between 200 and 300 km s^{-1} suggest, in addition to the internal motion of the nebula, a contribution of some other H I slabs which may be partially ionized by background UV radiation (Songaila, 1981) of the LMC.

We have overlayed the H I measures obtained by Rohlfs et al. (1984) onto the Hα + [N II] photograph by Davies et al. (Fig. 6). The overlay shows that the bubble is lying in a neutral plateau, with a column density 2 10^{20} cm^{-2} and a main velocity 243 km s^{-1}. A secondary velocity component occurs sporadically at 272 km s^{-1}.

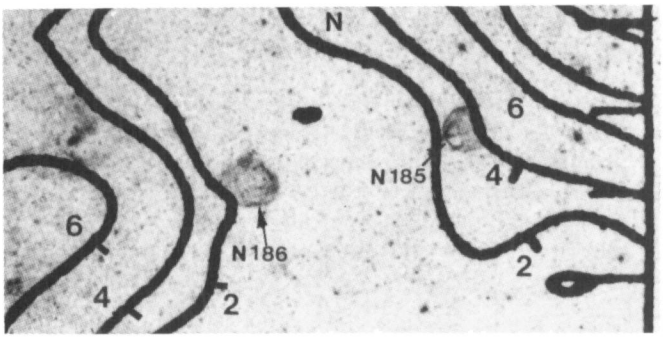

Fig. 6. H I contours superimposed on the Hα + [N II] image of the field covering N186 and N185

In their survey of giant LMC shells, Meaburn et al. (1984) found extensive and complex H I profiles at the positions and the immediate neighbourhood of the shells N186 and N185. They report faint wings and discrete H I components in the velocity range $V_{\rm Hel}$ 142–380 km s^{-1}, some of these components appearing to originate from local motions within the shells. They deduce the presence of a H I region with diameter larger than 490 pc for the component $V_{\rm Hel} \simeq 150$ km s^{-1}, and the possibility of H I regions of similar or larger extension for the other components.

Thus, the velocity field observed by us is possibly contaminated by faint emission originating in these H I slabs. However, Fig. 4 shows that the velocity dispersions are larger for the central parts of the bubble than at the edges where they have the minimum values. This implies that the internal velocity dispersions truly are due to internal motion of the nebular gas instead of motions of the H I slabs since otherwise the velocity dispersion should be independent of the location in the nebula. When interpreting the velocity dispersions as expansion we thus obtain the expansion velocity $V_{\rm exp} = 25 \pm 9$ km s^{-1}.

6. Interaction of SNRs

6.1. *An old SNR (N186E)*

In a previous work, Rosado (1986) explored the possibility that N186E is a bubble driven by a stellar wind. She concluded that N186E is in the phase of energy conservation which is rarely observed. However, at that time we did not know about the existence of Gr 3 and its influence on the nebula. The enhanced knowledge leads us to consider another physical state of the nebula.

The filamentary structure of the oval-shaped nebula, the off-center location of the stellar cluster Gr 3 and the lack of central early-type stars suggest that N186E may be an old SNR shell photoionized by the stars Gr 3. When adopting this interpretation, it is evident that N186E is not identified by radio observations: a SNR of the dimensions of N186E (147 pc × 109 pc) will have a non-thermal radio surface brightness below the detection limit of the Molonglo radio survey ($\Sigma_{408\,\rm GHz} \simeq 2\ 10^{-4}$ W m^{-2} Hz^{-1} sr^{-1}). On the other hand, the X-ray emission may still be significant.

If N186E is a SNR, it will be in the radiative phase and its expansion velocity approaches the sound speed of the ISM (Cs = 10 km s^{-1}). Our radial velocity observations confirm this picture since we have found indications of an expansion velocity $V_{\rm exp} = 25$ km s^{-1} (Sect. 5), while the similar bubble N185 has an expansion velocity 70 km s^{-1} (Rosado et al., 1982).

The pre-shock density, n_0, of N186E is determined from the rms electron density of the whole nebula and from the minimum observed shell thickness $\Delta R = 4$ pc. With n_e the electron density, the emission measure of the central part of the shell is: E.M. $= 2\Delta R n_e^2 = 2R(n_{\rm rms})^2$. Taking into account mass conservation and assuming that the mass of the shell is formed by ISM gas swept-up by the shock, and that no density inhomogeneities exist (clumps), then

$$n_{\rm rms}/n_0 = 1/3 \left(\frac{R}{\Delta R}\right)^{1/2}.$$

For the values of $n_{\rm rms} = 0.7$ cm^{-3} (Table 1) and ΔR given above, we obtain $n_0 = 0.4$ cm^{-3}. Because of the uncertainties of the fluxes and of the dimensions, the estimated range of values for the preshock density is 0.3 to 1.2 cm^{-3}.

The X-ray luminosity of N186E can be deduced from Einstein IPC fluxes and is $\sim 7\ 10^{34}$ erg s^{-1} (Chu, 1990). This is probably a lower limit because there may be additional X-ray emission near the interaction zone with the SNR N186D (see below Sect. 6.2). If N186E is a wind driven bubble, then the method described by Bachkarev and Lozinskaya (1985) gives for the expected X-ray flux

$$F_{\rm X} = 0.256\ 10^{-12}\, \zeta_{23}\, R^{17/7}\, d^{-2} \left(\frac{V_{\rm exp}}{100}\right)^{16/7} n_0^{10/7},$$

where ζ_{23} is a factor compiled by Bachkarev (1985), R is the shell radius in pc; d the distance, in kpc; $V_{\rm exp}$ the expansion velocity in km s^{-1} and n_0 the preshock density, in cm^{-3}. With the values obtained for N186E, $F_{\rm X} = 1.35\ 10^{-14}$ erg s^{-1} cm^{-2} when assuming $n_0 = 0.5$ cm^{-3}, and $7.46\ 10^{-16}$ erg s^{-1} cm^{-2} when assuming $n_0 = 0.1$ cm^{-3}. Thus the X-ray luminosity $L_{\rm X} = 4\pi d^2 F$ is $4.7\ 10^{33}$ erg s^{-1} or $2.6\ 10^{32}$ erg s^{-1}, respectively, if N186E is a pure wind driven bubble. These luminosities are well below the observed $7\ 10^{34}$ erg s^{-1} and hence, there must be an additional heating source, such as a SNR (Chu, 1990).

Thus N186E may be a fossil SNR.

Applying Chevalier's (1974) relations, the initial energy of the SNR N186E is 10^{51} erg and the age is $6.5\ 10^5$ yr. The oval shape of N186E may be explained by differences in densities along the NS and EW directions ($n_{\rm NS} > n_{\rm EW}$). We consider the NS dimension of 109 pc as representative for the SNR diameter (this will be justified below). In view of the physical state we believe that the SNR is susceptible of being rejuvenated because its internal pressure exceeds that of the ISM (Smith, 1977).

Another possibility is that an explosion of SN occurred inside a wind driven bubble excavated by the progenitor star(s). Ciotti and d'Ercole (1989) and Tenorio-Tagle et al. (1989) have shown that the presence of an excavated bubble increases the speed of evolution and causes an enhancement of the Hα emission, leading to an overestimation of the density and age derived from standard methods. It may be the case for N186E, but further observations and models are necessary for a better definition of the initial conditions.

6.2. *Interaction of two SNRs (N186D and N186E)*

We have established in Paper I the interaction of the SNR N186D with N186E.

The interaction of two SNRs has been studied theoretically by Ikeuchi (1978) and Jones et al. (1979) leading to an important understanding of the formation and development of tunnels of hot

gas in the ISM as suggested earlier by Cox and Smith (1974). When adopting the view that also N186E is a SNR, then we are probably observing the interaction of the old SNR, N186E ($t = 6.5\ 10^5$ yr) with a younger SNR, N186D.

Because of difficulties of the calibration as mentioned in Sect. 3, the revised average Hα surface brightness of N186D is $F_0(\mathrm{H}\alpha) = 0.40\ 10^{-5}\,\mathrm{erg\,cm^{-2}\,s^{-1}\,sr^{-1}}$ for the blue shifted velocity component. This flux $F_0(\mathrm{H}\alpha)$ indicates a rms density of $1.0\,\mathrm{cm^{-3}}$, a preshock density $n_0 = 1.5\,\mathrm{cm^{-3}}$, and an age $t_r = 7\ 10^4$ yr from Chevalier's relations for a velocity of $90\,\mathrm{km\,s^{-1}}$ as determined in Paper I.

At present both SNRs are in the radiative phase of evolution. The centers of the SNRs are separated by $\Delta = 54$ pc in the direction NS (this justifies our choice of the NS dimension of the SNR as being more significant).

The explosion of the SN which has formed N186D must have occured $t_0 = 5.8\ 10^5$ yr ago; we select t_0 as the origin of time. At t_0, N186E was still in the radiative phase of evolution. The time-dependent radius of N186E during the radiative phase is obtained from Chevalier's (1974) models. Our observations show that the original SN was more energetic than the SN considered in Chevalier's models ($E_0 = 10^{50}$ erg) so that we can only approximate the evolutionary law by scaling up Chevalier's model A to $E_0 = 6\ 10^{50}$ erg and a mean density $n_0 = 0.7\,\mathrm{cm^{-3}}$. Using the scaled model, we obtain for N186E the radius $R_0 = 50$ pc at the time t_0 when the SN of N186D exploded.

The encounter time t_E (i.e. the time of first contact of the SNRs, counted from t_0) is derived from the radius $R_1(t_E + t_0)$ of N186E and the radius $R_2(t_E)$ of N186D as $t_E = 2000$ yr and $R_2(t_E) = 6$ pc. At the encounter time, N186D was probably in the adiabatic phase since the swept up mass of a SNR of 6 pc diameter traveling through a medium of $n_0 = 1.5\,\mathrm{cm^{-3}}$ is larger than the ejected mass.

The conditions simulating well the situation of the encounter are those of Ikeuchi's (1978) model IV with the following parameters: $n_0 = 1\,\mathrm{cm^{-3}}$, $E_0 = 10^{51}$ erg, $t_0 = 9.4\ 10^5$ yr, $R_0 = 63.4$ pc and $\Delta = 80$ pc. The main difference of this model and our assumptions is the fact that at the time of encounter both SNRs were in the radiative phase. Consequently, the results of the model cannot be applied directly to our case and only some general conclusions may be derived.

Ikeuchi's model IV predicts the formation of a "dense plug" at the contact region of SNRs. This plug is later perforated and through the hole in the plug flows the hot gas from the younger SNR cavity into the older one. The plug disappears later and the lifetime of the older SNR is prolonged by 5% only whereas the evolution of the younger SNR is not affected at the side opposite to the interaction.

Although Jones et al. (1979) do not discuss the identical case, their comparison with Ikeuchi's model I indicates that the dense plug exists longer than predicted by Ikeuchi's models and that, even during the final state, the SNRs do not lose their identity.

Accounting for the differences between our observations and the parameters of the theoretical models, we arrive at the following picture:

– N186E and N186D are SNRs probably in interaction. This interaction may explain the asymmetry of the radial velocity field of N186D discussed in Paper I.

– The region of interaction (i.e. the plug) is the SW filament discussed in Paper I. This filament is denser than the remaining part of the shell, which is in agreement with the theoretical models.

– The monochromatic photographs and our radial velocity data show the feature of a plug, in agreement with the prediction of the models by Jones' et al. (1979). At the "age" of the plug, (i.e., the age of the younger SNR minus the encounter time) both SNRs have preserved their identity.

In Paper I and Sect. 2 of this paper we have explained the existence of three bright condensations of gas; two condensations are located inside the SW filament of N186D (at radial velocities of 240 and 170 $\mathrm{km\,s^{-1}}$ respectively) and another condensation at about 2 pc distance from the SW filament and coincident with the stellar cluster Gr 3. This condensation has a radial velocity of $229\,\mathrm{km\,s^{-1}}$.

The origin of these condensations is not clear. The condensations in the SW filament may result from Rayleigh-Taylor instabilities (RT) which have developed in this filament (identified as the plug); however, the possibility of shock-accelerated dense clumps of ISM cannot be excluded.

The models mentioned above do not predict the evolution of the dense plug nor comment on the generation and development of RT instabilities. However such instabilities are required for the formation of tunnels of hot gas in the ISM. According to Smith (1977), RT instabilities grow to a characteristic size $\lambda \sim 2\pi g t_{RT}^2$ (where g is the effective gravity $\gtrsim 4\,\mathrm{km\,s^{-1}}$ ($10^5\,\mathrm{yr^{-1}}$) and t_{RT} is the growth time of the instability in the linear regime). For $t_{RT} = 6.8\ 10^4$ yr (the age of the plug as derived above), the characteristic extension of the RT instability is approximately 1 pc. This scale is of the same order of magnitude as the dimension of the knots (1–5 pc) observed inside the plug (see Paper I and Table 1 of this paper). However, we cannot explain why these condensations exhibit so different velocities.

7. Conclusions

The radial velocity field of N186E is contaminated by low and high velocity components whose emission is due to photoionization of the LMC UV background radiation of two H I slabs located along the line of sight of this nebula. However, the pattern of the velocity dispersion is also in agreement with an expansion of $25\,\mathrm{km\,s^{-1}}$.

– The filamentary shape of this shell, the lack of early-type central stars, and the X-ray emission suggest this nebula to be an old SNR photoionized by the stellar cluster Gr 3. It is not clear whether a wind driven bubble existed before the SN explosion.

– The proximity of the SNRs N186D and N186E suggests that both SNRs are in interaction.

– The comparison between theoretical models for the interaction of SNRs and our observations suggests that the SW filament (Paper I) is a dense plug resulting from the interaction.

– The bright condensations found in the SW filament of N186D may be due to Rayleigh-Taylor instabilities within the plug or to the acceleration of already existing clumps of ISM. The gaseous condensation coinciding with Gr 3 may have another origin probably related to the stellar cluster.

We believe that the interaction of SNRs is quite frequent, though generally overlooked, because in order to be observable it is necessary that the old SNR shell is illuminated by internal hot stars, as being the case for N186E.

Acknowledgements. We acknowledge Dr. Chu for her fruitful comments. We thank Mr. J. A. Fort for technical assistance during the observations, and Mr. P. Joulié for the design of the focal reducer.

References

Bachkarev, N.G.: 1985, *Sov. Astron.* **29**, 509
Bachkarev, N.G., Lozinskaya, T.A.: 1985, *Sov. Astron.* **29**, 60
Boulesteix, J., Georgelin, Y.P., Marcelin, M., Monnet, G.: 1984, *Instrumentation in Astronomy*, eds. V.A. Boksenberg, D.L. Crawford, *Proc. SPIE* **445**, 37
Caplan, J.: 1972, *Astron. Astrophys.* **18**, 408
Caplan, J., Deharveng, L.: 1983, *The Messenger* **32**, 3
Caplan, J., Deharveng, L.: 1985, *Astron. Astrophys. Suppl.* **62**, 63
Chevalier, R.A.: 1974, *Astrophys. J.* **188**, 501
Chu, Y.H.: 1983, *Astrophys. J.* **269**, 202
Chu, Y.H.: 1990 (private communication)
Ciotti, L., d'Ercole, A.: 1989, *Astron. Astrophys.* **215**, 347
Cox, D.P., Smith, B.W.: 1974, *Astrophys. J. Letters* **189**, L105
Davies, R.D., Elliott, K.H., Meaburn, J.: 1976, *Monthly Notices Roy. Astron. Soc.* **81**, 89 (DEM)
Feast, M.W.: 1984, *IAU Symp.* **108**, 157
Graham, J.R., Evans, A., Albinson, J.S., Bode, M.F., Meikle, W.P.S.: 1987, *Astrophys. J.* **319**, 126
Greve, A., Van Genderen, A.M., Laval, A., Van Driel, W., Prein, J.J.: 1988, *Astron. Astrophys. Suppl.* **74**, 167
Henize, K.G.: 1956, *Astrophys. J. Suppl.* **2**, 315
Ikeuchi, S.: 1978, *Publ. Astron. Soc. Japan* **30**, 563
Jones, E.C., Smith, B.W., Straka, W.C., Kodis, J.W., Guitar, H.: 1979, *Astrophys. J.* **232**, 129
Lasker, B.M.: 1976, *RGO Bull.* no. **182**, p. 185
Lasker, B.M.: 1977, *Publ. Astron. Soc. Pacific* **89**, 474
Lasker, B.M.: 1979, *Publ. Astron. Soc. Pacific* **91**, 153
Lasker, B.M.: 1980, *Astrophys. J.* **239**, 65
Laval, A., Boulesteix, J., Georgelin, Y.M., Georgelin, Y.P., Marcelin, M.: 1987, *Astron. Astrophys.* **175**, 199
Laval, A., Rosado, M., Boulesteix, J., Georgelin, Y.P., Marcelin, M., Monnet, G., Le Coarer, E.: 1989, *Astron. Astrophys.* **208**, 230 (Paper I)
Marcelin, M., Boulesteix, J., Georgelin, Y.P.: 1985, *Nature* **316**, 705
Mathewson, D.S., Ford, V.L., Dopita, M.A., Tushy, I.R., Long, K.S., Helfand, D.J.: 1983, *Astrophys. J. Suppl.* **51**, 345
Meaburn, J., McGee, K.X., Newton, L.M.: 1984, *Monthly Notices Roy. Astron. Soc.* **206**, 705
Meaburn, J.: 1987, *Monthly Notices Roy. Astron. Soc.* **229**, 457
Nandy, K., Morgan, D.H., Willis, A.J., Wilson, R., Gondhalekar, P.M.: 1981, *Monthly Notices Roy. Astron. Soc.* **196**, 955
Panagia, N.: 1973, *Astron. J.* **78**, 929
Rosado, M.: 1986, *Astron. Astrophys.* **160**, 211
Rosado, M.: 1989, *Rev. Mexicana Astron. Astrofis.* **18**, 105
Rohlfs, K., Kreitschmann, J., Siegmann, B.C., Feitzinger, J.V.: 1984, *Astron. Astrophys.* **137**, 343
Rousseau, J., Martin, N., Prévot, L., Rebeirot, E., Robin, A., Brunet, J.P.: 1978, *Astron. Astrophys.* **31**, 243
Sanduleak, N.: 1970, *Cerro-Toldo, Inter-American Observatory Contribution* No. **89**
Sanduleak, N., Philip, A.G.D.: *Publication Warner and Swasey Observatory*, Vol. **2**, no. **5**
Smith, B.W.: 1977, *Astrophys. J.* **211**, 404
Songaila, A.: 1981, *Astrophys. J.* **248**, 945
Stasińska, G.: 1982, *Astron. Astrophys. Suppl.* **48**, 299
Tenorio-Tagle, G., Bodenheimer, P., Franco, J., Rozyczka, M.: 1990, *Monthly Notices Roy. Astron. Soc.* **244**, 563